Am J Physiol Renal Physiol 303: F483–F491, 2012.
First published May 30, 2012; doi:10.1152/ajprenal.00062.2012.

CALL FOR PAPERS | *Integrative Aspects of Renal Endocrinology*

Differential effects of extracellular ATP on chloride transport in cortical collecting duct cells

Madhumitha Rajagopal,[1] Paru P. Kathpalia,[1] Jonathan H. Widdicombe,[2] and Alan C. Pao[1,3]

[1]*Division of Nephrology, Department of Medicine, Stanford University, Stanford, California;* [2]*Department of Physiology and Membrane Biology, University of California, Davis, California; and* [3]*Veterans Affairs Palo Alto Health Care System, Palo Alto, California*

Submitted 31 January 2012; accepted in final form 24 May 2012

Rajagopal M, Kathpalia PP, Widdicombe JH, Pao AC. Differential effects of extracellular ATP on chloride transport in cortical collecting duct cells. *Am J Physiol Renal Physiol* 303: F483–F491, 2012. First published May 30, 2012; doi:10.1152/ajprenal.00062.2012.—Extracellular ATP in the cortical collecting duct can inhibit epithelial sodium channels (ENaC) but also stimulate calcium-activated chloride channels (CACC). The relationship between ATP-mediated regulation of ENaC and CACC activity in cortical collecting duct cells has not been clearly defined. We used the mpkCCD$_{c14}$ cortical collecting duct cell line to determine effects of ATP on sodium (Na^+) and chloride (Cl^-) transport with an Ussing chamber system. ATP, at a concentration of 10^{-6} M or less, did not inhibit ENaC-mediated short-circuit current (I_{sc}) but instead stimulated a transient increase in I_{sc}. The macroscopic current-voltage relationship for ATP-inducible current demonstrated that the direction of this ATP response changes from positive to negative when transepithelial voltage (V_{te}) is clamped to less than −10 mV. We hypothesized that this negative V_{te} might be found under conditions of aldosterone stimulation. We next stimulated mpkCCD$_{c14}$ cells with aldosterone (10^{-6} M) and then clamped the V_{te} to −50 mV, the V_{te} of aldosterone-stimulated cells under open-circuit conditions. ATP (10^{-6} M) induced a transient increase in negative clamp current, which could be inhibited by flufenamic acid (CACC inhibitor) and BAPTA-AM (calcium chelator), suggesting that ATP stimulates Cl^- absorption through CACC. Together, our findings suggest that the status of ENaC activity, by controlling V_{te}, may dictate the direction of ATP-stimulated Cl^- transport. This interplay between aldosterone and purinergic signaling pathways may be relevant for regulating NaCl transport in cortical collecting duct cells under different states of extracellular fluid volume.

P2Y receptor; CACC; ENaC

THE CORTICAL COLLECTING DUCT of the kidney plays a critical role in maintaining sodium chloride (NaCl) balance by responding to hormonal cues for fine-tuning of urinary NaCl excretion. For example, under conditions of extracellular fluid (ECF) volume depletion, aldosterone and arginine vasopressin (AVP) activate the epithelial Na^+ channel (ENaC), the principal ion channel responsible for Na^+ absorption in the collecting duct (4, 11, 25). Conversely, under conditions of high-dietary NaCl intake, extracellular nucleotides such as adenosine triphosphate (ATP) inhibit ENaC (16, 17, 34), limiting development of ECF volume expansion and hypertension (17, 22). While regulation of ENaC-mediated Na^+ transport is widely recognized to be a major determinant of ECF volume and blood pressure, regulation of Cl^- transport in the collecting duct may also contribute to the maintenance of NaCl balance (10, 24, 32).

Although recent studies support the in vivo role for extracellular ATP in inhibiting ENaC-mediated Na^+ absorption in the cortical collecting duct, ATP also stimulates Cl^- secretion in several model systems (8, 9, 20, 35). For example, in M1 cortical collecting duct cells, ATP decreases ENaC-mediated Na^+ absorption and also increases Cl^- secretion through calcium-activated Cl^- channels (CACC) (6). Thus, ATP likely has differential effects on NaCl transport in cortical collecting duct cells under specific physiological contexts. However, the relationship between ATP-mediated regulation of ENaC and CACC in cortical collecting duct cells has not been well-characterized.

To define the conditions that promote ATP-mediated stimulation of Cl^- transport in cortical collecting duct cells, we used the mpkCCD$_{c14}$ cortical collecting duct cell line as a model system and measured direct effects of extracellular ATP on NaCl transport in Ussing chambers. We found that ATP induced a multiphasic short-circuit current (I_{sc}) response, comprised of an initial transient peak followed by a sustained decrease in I_{sc}. The sustained phase of the ATP response reflected an inhibition of ENaC activity, which was only observed when cells were treated with ATP concentrations greater than 10^{-6} M. In contrast, the transient phase of the ATP response was observed even when cells were treated with ATP concentrations less than 10^{-6} M.

We hypothesized that this transient phase of the ATP response reflects a stimulation of Cl^- transport, possibly mediated through CACC. We generated a macroscopic current-voltage curve for the transient phase of the ATP response and observed that the direction of this response changes from positive to negative when transepithelial voltage (V_{te}) is clamped to less than −10 mV. We further hypothesized that this negative current signifies ATP-inducible Cl^- absorption, which might be found under conditions of aldosterone stimulation. To test this, we treated mpkCCD$_{c14}$ cells with aldosterone and clamped the V_{te} to −50 mV, which was the V_{te} across aldosterone-stimulated cells under open-circuit conditions. We then characterized the putative CACC transport pathways responsible for ATP-stimulated Cl^- absorption under these conditions.

METHODS

Cell culture. Immortalized mouse kidney cortical collecting duct (mpkCCD$_{c14}$) cells, kindly provided by Dr. Alain Vandewalle, were maintained as previously described (3, 30). mpkCCD$_{c14}$ cells were

Address for reprint requests and other correspondence: A. C. Pao, Div. of Nephrology, Dept. of Medicine, Stanford Univ., 780 Welch Rd., Suite 106, Palo Alto, CA 94304 (e-mail: paoman@stanford.edu).

subcultured onto collagen-coated Snapwell-permeable supports (0.4-μm-pore size, Costar, Cambridge, MA) and grown in defined medium until transepithelial resistance (R_{te}) reached values greater than 4,000 Ω·cm^2, as measured with an EVOM "chopstick" voltmeter (World Precision Instruments, Sarasota, FL). Cells were then switched to supplement and serum-free media for 48 to 72 h. Cells were treated with aldosterone (10^{-6} M) for a period of 4 h before being mounted on the Ussing chamber.

Ussing chamber measurements. Cell monolayers were mounted between the Lucite half chambers of the Ussing chamber (Physiological Instruments, San Diego, CA) for electrophysiological studies, as described previously (19, 21). Cell monolayers were bathed in Krebs-Henseleit solution (in mM: 140 NaCl, 25 $NaHCO_3$, 5 KCl, 5 glucose, 2 $CaCl_2$, and 1 $MgCl_2$) and gassed with a mixture of 95% O_2-5% CO_2. V_{te} across cell monolayers was clamped to 0 mV, and a set voltage pulse of 1 mV was applied across cell sheets for 200 ms every 20 s. I_{sc} and R_{te} across cell monolayers were continuously recorded using Acquire and Analyze Software (Physiological Instruments).

To examine effects of extracellular nucleotides on I_{sc}, ATP (10^{-5} M) was added to the apical side of cell monolayers. In some experiments, amiloride (10^{-5} M) was added to cell monolayers before apical addition of ATP to isolate independent effects of ATP on cation (ENaC-mediated) and anion transport. In other experiments, a dose response for ATP-stimulated I_{sc} was performed by treating cell monolayers with a range of ATP concentrations (10^{-8} to 10^{-4} M).

To generate a macroscopic current-voltage curve, ATP-inducible clamp current (I_{clamp}^{ATP}) was measured at various voltages (−50, −25, −10, 0, or +25 mV) across cell monolayers. To establish Cl^- as an anion involved in ATP-stimulated anion transport, Cl^- was substituted with gluconate or sulfate in Krebs-Henseleit solution, while bicarbonate was substituted with HEPES to buffer the solution. The concentrations of all other ions were kept constant. Cell monolayers were then voltage clamped to −50 mV and stimulated with ATP (10^{-6} M). To rule out basolateral potassium (K^+) transport as an underlying mechanism for I_{clamp}^{ATP}, $BaCl_2$ (10^{-3} M) was added to the basal side of cell monolayers before apical addition of ATP in some experiments.

Pharmacological agents. A series of pharmacological agents was used to verify the involvement of P2Y receptor signaling pathways in ATP-stimulated anion transport. Some cell monolayers were exposed to the P2Y receptor blocker suramin (5×10^{-4} M) before ATP stimulation. Other cell monolayers were pretreated with the calcium (Ca^{2+}) chelator BAPTA-AM (5×10^{-5} M). To identify the classes of ion channels or transporters responding to P2Y receptor activation, CFTR inhibitor-172 (10^{-5} M, Sigma) was used to block cystic fibrosis transmembrane conductance regulator (CFTR), and flufenamic acid (FFA; 2×10^{-4} M, Sigma) was used to block CACC.

Reverse-transcriptase PCR. mpkCCD$_{c14}$ cells were grown to resistance on permeable supports, and total RNA was harvested using an RNeasy Mini Kit (Qiagen, Valencia, CA) according to the manufacturer's instructions. Mouse brain and kidney total RNA were obtained from Zyagen (San Diego, CA) to serve as positive controls. Reverse-transcriptase (RT) reactions were performed according to the manufacturer's instructions (New England BioLabs, Ipswich, MA). Thermal cycling parameters were the following: incubation at 98°C for 30 s followed by 35 cycles at 98°C for 10 s, 52°C for 10 s, 72°C for 50 s, and then a final extension at 72°C for 5 min.

PCR primers were designed and used for detecting gene amplification of TMEM16A and bestrophin-1 (7, 14). PCR primers were also used for detecting expression of actin as a loading control. Specificity of each set of primers was confirmed by BLAST search against GenBank and by direct sequencing of PCR products. The primer sequences were as follows: mouse TMEM16A forward: 5′-GGTGTCGGGTTTGTGAAGAT-3′, mouse TMEM16A reverse: 5′-TGCACGTTGTTCTCTTCAGG-3′; mouse bestrophin-1 forward: 5′-AGGACGATGATGATTTTGAGACTAA-3′, mouse bestrophin-1 reverse: 5′-CTTTCTGGTTTTTCTGGTTGGCATC-3′.

PCR products were resolved using a 1% agarose gel-dissolved Tris-Acetate EDTA buffer and visualized with ethidium bromide.

ATP determination assay. Medium from the apical side of mpkCCDc14 cell monolayers was replaced with 150 μl of phosphate-buffered saline. One hour after medium replacement, AVP (10^{-9} M, Tocris Biosciences) or vehicle was added to cell monolayers. Ten minutes later, PBS from the apical side of the cell monolayers was gently removed. ATP concentration in the PBS solution from AVP- and vehicle-treated cell monolayers was measured with an ATP Determination Kit (Invitrogen) and a luminometer (Glomax 20/20, Promega, Madison, WI).

Statistics. Statistical analyses for comparisons between different treatment groups of mpkCCD$_{c14}$ cells were performed using paired or unpaired two-tailed Student's *t*-tests. Differences were considered to be significant at $P < 0.05$.

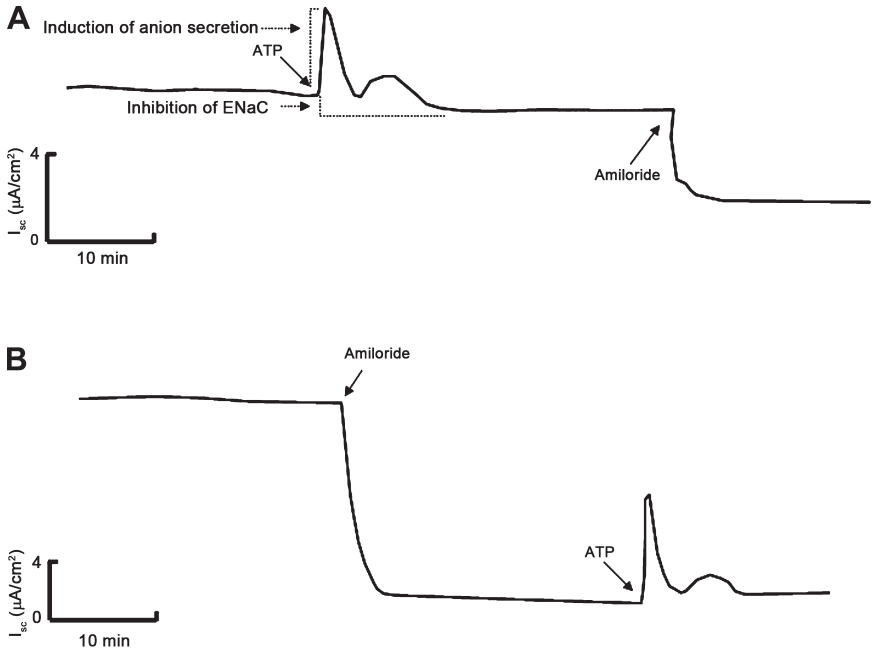

Fig. 1. Effects of extracellular ATP on short-circuit current in mpkCCD$_{c14}$ cells. *A*: representative trace of a short-circuit current (I_{sc}) response to addition of ATP (10^{-5} M) to the apical side of mpkCCD$_{c14}$ cell monolayers; amiloride indicates addition of amiloride (10^{-5} M) to the apical side. Addition of ATP caused a response consisting of an initial sharp peak, a second lower peak, followed by a sustained fall in I_{sc}. The sustained fall in I_{sc} reached a level that was lower than that of baseline I_{sc}. *B*: representative trace of a I_{sc} response when ATP (10^{-5} M) was added after addition of amiloride (10^{-5} M). Pretreatment of mpkCCD$_{c14}$ cell monolayers with amiloride did not influence the initial peak in I_{sc}, but it did eliminate the sustained fall in I_{sc}.

RESULTS

ATP induces anion secretion in mpkCCD$_{c14}$ cells. We first tested the effect of apical application of ATP (10^{-5} M) on I_{sc} across mpkCCD$_{c14}$ cell monolayers. We found that ATP induced a multiphasic response comprised of an initial transient peak, a second lower peak, and then a sustained decrease in I_{sc} (Fig. 1*A*). The sustained decrease in I_{sc} fell below the baseline level of I_{sc}, suggesting that ATP inhibits ENaC-mediated Na^+ transport. To confirm this, we evaluated the ATP response in the presence of amiloride, a specific ENaC inhibitor. Amiloride (10^{-5} M) altered the ATP response by eliminating the sustained decrease in I_{sc}, indicating that this component of the I_{sc} response is due to ATP-mediated inhibition of ENaC-mediated Na^+ absorption (Fig. 1*B*). In contrast, the initial transient peak in I_{sc} of the ATP response was resistant to amiloride inhibition, suggesting that this component of the I_{sc} response might be due to ATP-stimulated anion secretion.

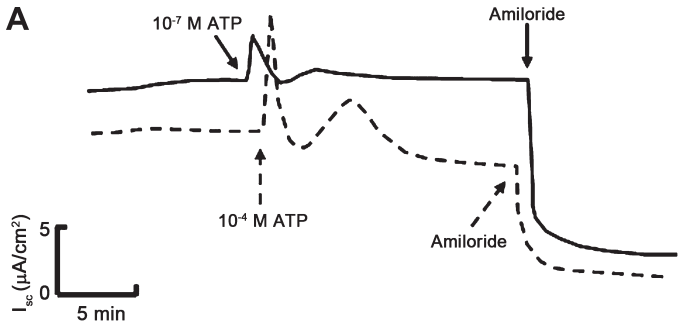

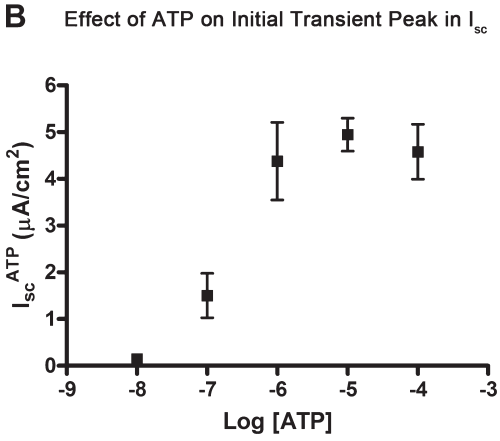

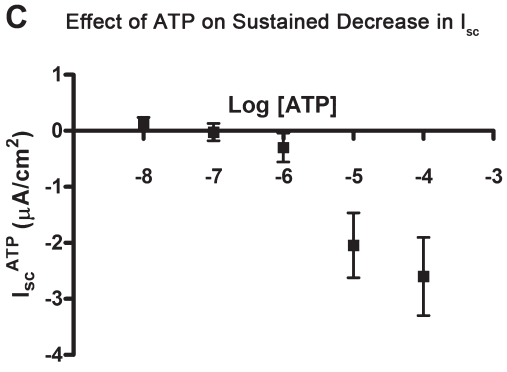

Fig. 2. ATP dose-response curve in mpkCCD$_{c14}$ cells. *A*: superimposed representative I_{sc} traces showing the effect of ATP on I_{sc} at a concentration of 10^{-7} M (solid line) or 10^{-4} M (dashed line); amiloride indicates addition of amiloride (10^{-5} M) to the apical side of mpkCCD$_{c14}$ cell monolayers. *B*: dose response for ATP-induced initial peak in I_{sc} (I_{sc}^{ATP}). *C*: dose response for ATP-induced sustained decrease in I_{sc} (I_{sc}^{ATP}). Data are means ± SE (n = 6 filters each).

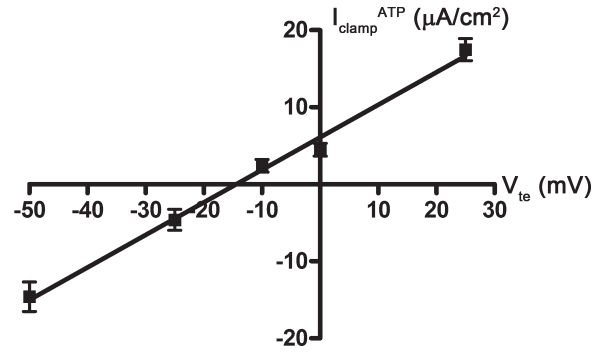

Fig. 3. Macroscopic current-voltage (*I-V*) curve for ATP-inducible current in mpkCCD$_{c14}$ cells. mpkCCD$_{c14}$ cell monolayers were mounted in an Ussing chamber and clamped to different voltages (−50, −25, −10, 0, and +25 mV). At each voltage (V_{te}), cell monolayers were treated with ATP (10^{-5} M), and the resulting clamp current (I_{clamp}^{ATP}) was measured. Data are means ± SE (n = 6–7 filters each).

We next performed a dose response for the initial transient peak and the sustained decrease in I_{sc} of the ATP response. We added ATP (10^{-8} to 10^{-4} M) to the apical surface of aldosterone-stimulated mpkCCD$_{c14}$ cells and observed that, at concentrations between 10^{-5} and 10^{-4} M, ATP induced a multiphasic response (dashed line, Fig. 2*A*); however, at concentrations between 10^{-7} and 10^{-6} M, ATP stimulated an isolated transient peak in I_{sc} without a subsequent decrease in sustained I_{sc} (solid line, Fig. 2*A*). In a series of experiments, we quantified the transient and sustained I_{sc} responses in aldosterone-stimulated mpkCCD$_{c14}$ cells treated with ATP at concentrations ranging from 10^{-8} and 10^{-4} M and generated a dose-response profile for each phase of the ATP response. We found that the transient and sustained I_{sc} response profiles were distinct: the transient increase in I_{sc} was observed with ATP greater or equal to 10^{-7} M (Fig. 2*B*), whereas the sustained

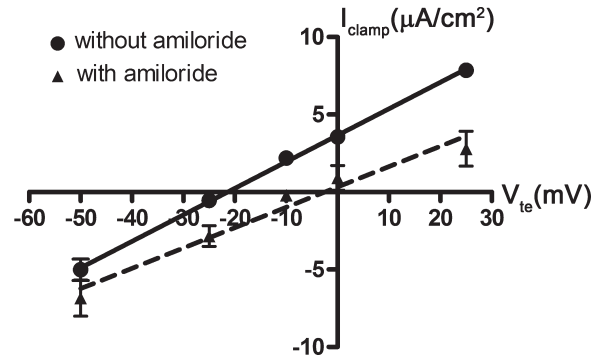

Fig. 4. Macroscopic *I-V* curves in mpkCCD$_{c14}$ cells. Shown here are 2 macroscopic *I-V* curves in the presence (dashed line) and absence of amiloride (solid line). Cell monolayers were treated with vehicle control or aldosterone (10^{-6} M) for 4 h and then mounted in an Ussing chamber. Cell monolayers were clamped to different voltages (−50, −25, −10, 0, and +25 mV). At each voltage (V_{te}), the resulting clamp current (I_{clamp}) in cells was measured. ATP was not added to cells in these experiments. Data are means ± SE (n = 4–5 filters each).

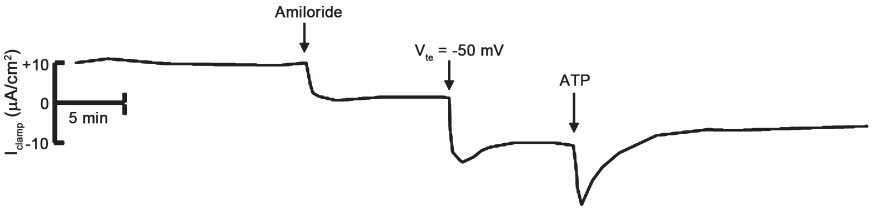

Fig. 5. Effect of extracellular ATP on clamp current in mpkCCD$_{c14}$ cells at a transepithelial voltage of −50 mV. Representative I_{clamp} trace of cells treated with amiloride (10^{-5} M), clamped to a transepithelial voltage (V_{te}) of −50 mV, and then treated with ATP (10^{-6} M).

decrease in I_{sc} was observed with ATP concentrations greater or equal to 10^{-5} M (Fig. 2*C*).

ATP also induces anion absorption in mpkCCD$_{c14}$ cells. We hypothesized that the transient phase of the ATP response reflects a stimulation of anion transport, and specifically, Cl^- transport. Using a similar cortical collecting duct cell line, Cuffe and colleagues (6) previously demonstrated that ATP stimulates CACC-mediated Cl^- secretion under short-circuit conditions. We generated a macroscopic current-voltage curve for this transient phase of the ATP response by plotting the change in I_{sc} in the presence and absence of ATP at each clamped voltage (−50, −25, −10, 0, or +25 mV). We also examined this relationship in the presence of amiloride (10^{-5} M) so that we could isolate the effects of ATP on anion transport. ATP (10^{-5} M) induced an increase in positive I_{sc} when V_{te} was clamped to greater than −10 mV, whereas ATP induced an increase in negative I_{sc} when V_{te} was clamped to less than −10 mV (Fig. 3). The negative I_{sc} response likely represents an increase in anion absorption, and not cation secretion, because these experiments were done in the presence of amiloride.

We hypothesized that this negative current signifies ATP-inducible anion absorption, which might operate under conditions of aldosterone stimulation. Aldosterone is the prototypic

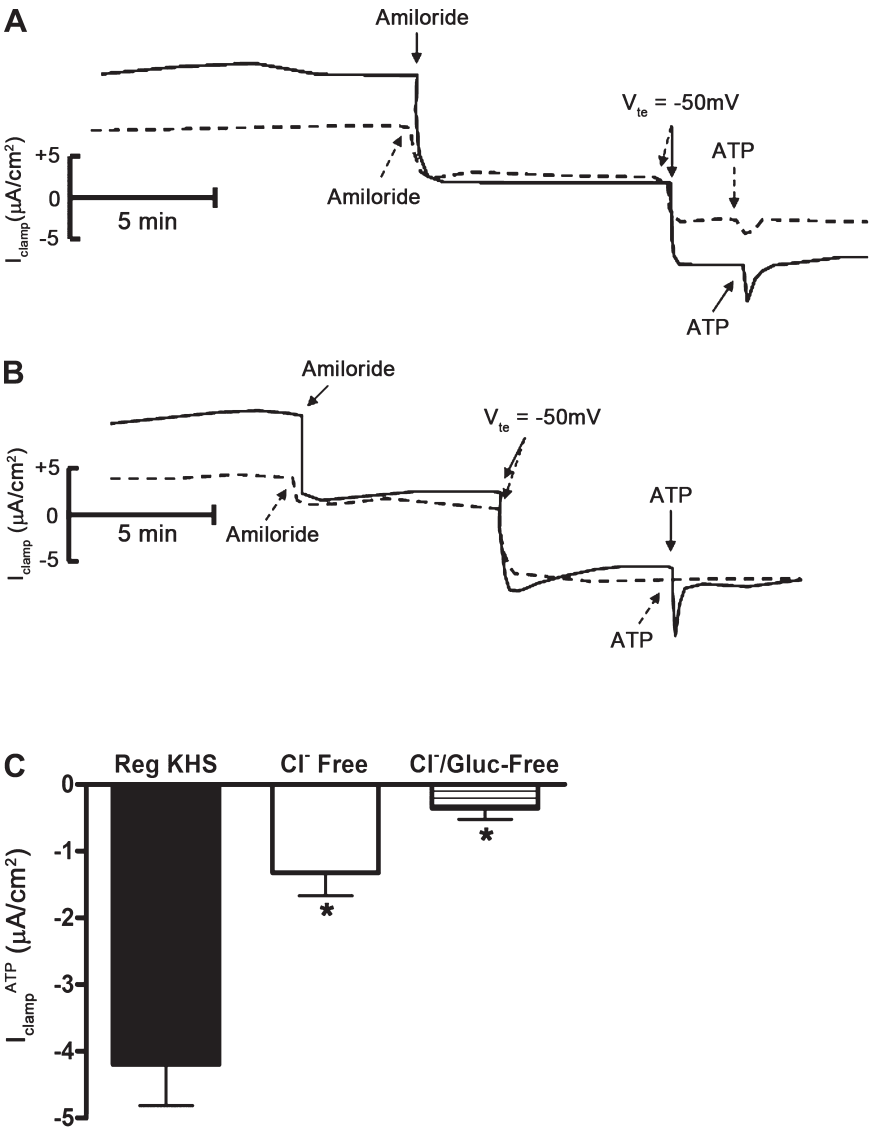

Fig. 6. Effect of chloride and bicarbonate substitution in the bath solution on ATP-inducible clamp current in mpkCCD$_{c14}$ cells. *A*: superimposed I_{clamp} traces of cell monolayers bathed in regular Krebs-Henseleit solution (solid trace) or in Krebs-Henseleit solution in which chloride (Cl^-) and bicarbonate (HCO_3^-) were replaced with gluconate and HEPES (dashed trace). Amiloride indicates addition of amiloride (10^{-5} M) to the apical bath; V_{te} indicates clamp of transepithelial voltage to −50 mV; ATP indicates addition of ATP (10^{-6} M) to the apical bath. *B*: superimposed I_{clamp} traces of cell monolayers bathed in regular Krebs-Henseleit solution (solid trace) or in Krebs-Henseleit solution in which Cl^- and HCO_3^- were replaced with sulfate and HEPES (dashed trace). *C*: quantitation of I_{clamp} values in response to apical addition of ATP to cell monolayers bathed in regular Krebs-Henseleit solution (Reg KHS), in KHS in which Cl^- and HCO_3^- were replaced with gluconate and HEPES (Cl^- free), or in KHS in which Cl^- and HCO_3^- were replaced with sulfate and HEPES (Cl^-/Gluc-Free; $n = 12$ filters). *$P < 0.05$.

stimulator of ENaC activity in the cortical collecting duct, and stimulation of ENaC activity generates a lumen negative V_{te}. To verify that aldosterone might provide the electrical driving force for ATP-stimulated anion absorption, we compared the V_{te} of mpkCCD$_{c14}$ cell monolayers treated with either vehicle or aldosterone (10^{-6} M for 4 h) under open-circuit conditions. As expected, aldosterone induced a drop in V_{te} from -10 mV (vehicle) to -50 mV, which corresponds to V_{te} of native cortical collecting duct under baseline and aldosterone-stimulated conditions, respectively (26–29).

ATP activates P2Y receptors and stimulates Cl^- absorption through CACC in mpkCCD$_{c14}$ cells. To evaluate ATP-inducible anion absorption, we used a strategy in which we clamped aldosterone-stimulated mpkCCD$_{c14}$ cells to a V_{te} of -50 mV, the V_{te} of aldosterone-stimulated cells under open-circuit conditions, before ATP treatment. We first verified that the current resulting from a V_{te} of -50 mV would be identical regardless of whether cells were treated with amiloride. We generated macroscopic current-voltage curves, in the absence of ATP (Fig. 4). The solid and dashed lines show the current-voltage relationship in the absence and presence of amiloride, respectively. These two lines intersect when the voltage is clamped to -50 mV, indicating that, at this voltage, the electrochemical gradient does not further drive ENaC-mediated ion transport.

We next treated mpkCCD$_{c14}$ cells with aldosterone (10^{-6} M) for 4 h, added amiloride (10^{-5} M) to the apical surface, and clamped the V_{te} to -50 mV. Under these conditions, addition of ATP (10^{-6} M) to the apical surface induced an additional transient increase in negative I_{clamp}^{ATP} (Fig. 5). Since these experiments were done in the presence of amiloride, the increase in negative I_{sc} most likely represents stimulation of Cl^- absorption. We confirmed this with ion substitution experiments: substitution of Cl^- with gluconate or sulfate largely reduced or eliminated I_{clamp}^{ATP}, respectively (Fig. 6). To rule out basolateral K^+ transport as an underlying mechanism for I_{clamp}^{ATP}, we added $BaCl_2$ (a broad spectrum K^+ channel inhibitor) to the basal side of mpkCCD$_{c14}$ cells before ATP addition. Basal application of $BaCl_2$ (10^{-3} M) did not inhibit I_{clamp}^{ATP} (data not shown), indicating that basolateral Cl^- efflux, rather than K^+ influx, is responsible for I_{clamp}^{ATP}.

To identify the chloride channels involved in ATP-mediated Cl^- absorption, we repeated this series of experiments in the presence of CFTR inhibitor-172 (a selective CFTR inhibitor) or FFA (a CACC inhibitor) before addition of ATP. Treatment of cells with CFTR inhibitor-172 (10^{-5} M) had no effect on I_{clamp}^{ATP} (data not shown); however, treatment of cells with FFA (2×10^{-4} M) inhibited I_{clamp}^{ATP} (Fig. 7), suggesting that ATP stimulates Cl^- absorption through CACC. To confirm the involvement of CACC with I_{clamp}^{ATP}, we used the Ca^{2+} chelator BAPTA-AM to decrease the intracellular Ca^{2+} concentration in mpkCCD$_{c14}$ cells. Pretreatment of cells with BAPTA-AM (5×10^{-5} M) eliminated I_{clamp}^{ATP} (Fig. 8).

The P2Y receptor system initiates ATP signaling in cortical collecting duct cells (6, 16, 17). To verify the involvement of P2Y receptors in I_{clamp}^{ATP}, we voltage-clamped mpkCCD$_{c14}$ cells to -50 mV and treated cells with suramin (a broad spectrum P2Y receptor blocker) before apical addition of ATP (10^{-6} M). Pretreatment of cells with suramin (5×10^{-4} M) blocked I_{clamp}^{ATP} (Fig. 9).

mpkCCD$_{c14}$ cells express TMEM16A and bestrophin-1. The molecular identity of CACC in epithelial cells has proven to be elusive. Two potential molecular candidates for CACC have recently emerged: TMEM16A (5, 23, 33) and bestrophin-1 (1, 2). TMEM16A encodes a membrane protein that mediates CACC current when heterologously expressed in

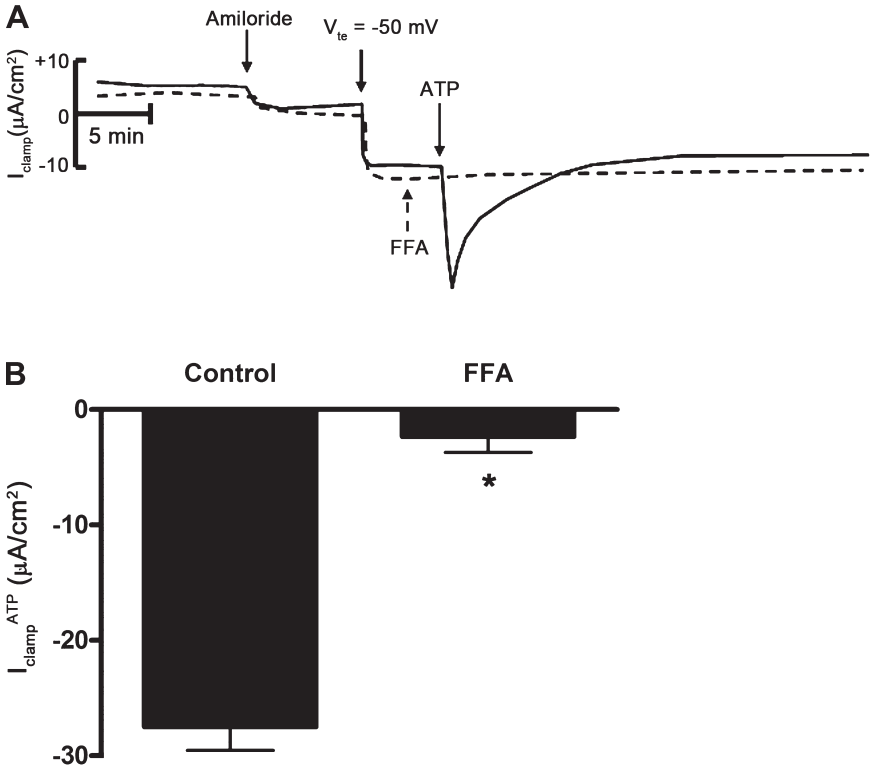

Fig. 7. Flufenamic acid (FFA) inhibits ATP-inducible clamp current in mpkCCD$_{c14}$ cells. *A*: superimposed I_{clamp} traces of cell monolayers treated with amiloride (10^{-5} M), clamped to a transepithelial voltage (V_{te}) of -50 mV, and then treated with vehicle control (solid trace) or FFA (dashed trace). FFA indicates addition of FFA (2×10^{-4} M) to the apical side; ATP indicates addition of ATP (10^{-6} M ATP) to the apical side. *B*: quantitation of I_{clamp} values in response to apical addition of ATP in control filters or in filters pretreated with FFA to the apical side ($n = 6$ filters). *$P < 0.05$.

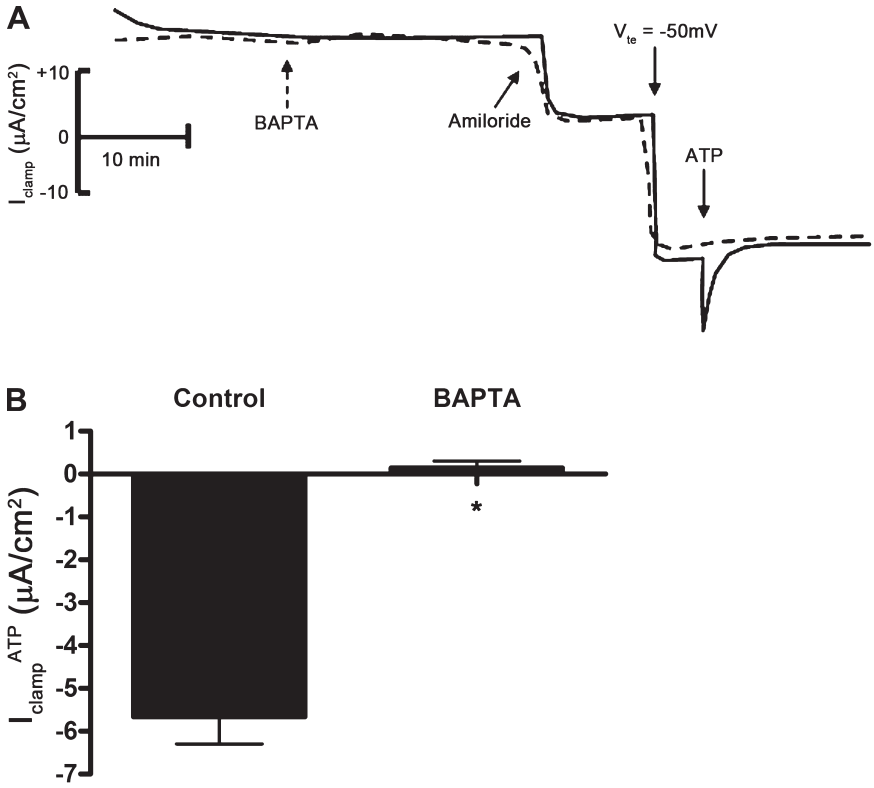

Fig. 8. BAPTA-AM inhibits ATP-inducible clamp current in mpkCCD$_{c14}$ cells. *A*: superimposed I_{clamp} traces of cell monolayers treated with vehicle control (solid trace) or BAPTA-AM (dashed trace). BAPTA indicates addition of BAPTA-AM (5×10^{-5}) to both sides; amiloride indicates addition of amiloride (10^{-5} M) to the apical side; V_{te} indicates clamp of transepithelial voltage to −50 mV; ATP indicates addition of ATP (10^{-6} M) to the apical side. *B*: quantitation of I_{clamp} values in response to apical addition of ATP in control filters or in filters pretreated with BAPTA-AM (BAPTA) to the apical side ($n = 12$ filters). *$P < 0.05$.

HEK293 cells (5, 23, 33). Knockdown of TMEM16A expression in pancreatic and bronchial epithelial cells also inhibits CACC activity (5). Bestrophin-1 is the product of VMD2 gene, mutations of which cause early-onset autosomal dominant macular dystrophy of the retina or Best disease (15). When transfected with bestrophin-1, HEK293 cells demonstrate ATP-stimulated CACC activity. Knockdown of bestrophin-1 expression in human airway cells also leads to suppression of ATP-inducible Cl^- currents (1).

To document the expression of molecular candidates for CACC in mpkCCD$_{c14}$ cells, we next performed RT-PCR to evaluate mRNA expression of TMEM16A and bestrophin-1 (1, 2, 5, 12). We used a PCR-based approach because we anticipated that expression of genes encoding CACC in mpkCCD$_{c14}$

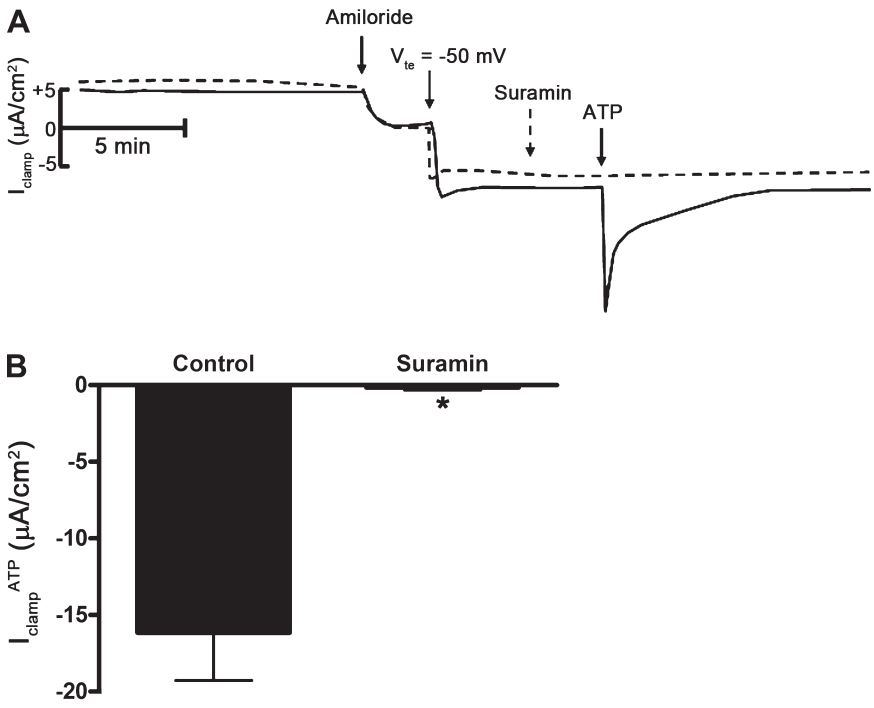

Fig. 9. Suramin inhibits ATP-inducible clamp current in mpkCCD$_{c14}$ cells. *A*: superimposed I_{clamp} traces of cell monolayers treated with vehicle control (solid trace) or the broad spectrum P2Y receptor blocker suramin (dashed trace). Suramin indicates addition of suramin (5×10^{-4} M) to both sides; amiloride indicates addition of amiloride (10^{-5} M) to the apical side; V_{te} indicates clamp of transepithelial voltage to −50 mV; ATP indicates addition of ATP (10^{-6} M) to apical side. *B*: quantitation of I_{clamp} values in response to apical addition of ATP in control filters or in filters pretreated with suramin to the apical side ($n = 12$ filters each). *$P < 0.05$.

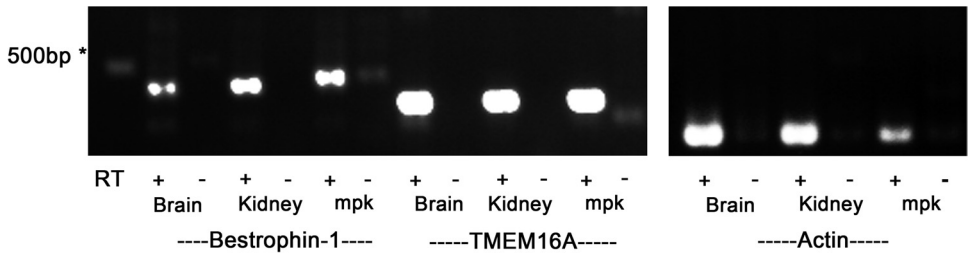

Fig. 10. Expression of TMEM16A and bestrophin-1 mRNA in mpkCCD$_{c14}$ cells. Photograph of gel showing PCR amplification products in mouse brain and kidney tissue (positive controls) and in mpkCCD$_{c14}$ cells (mpk) after reverse transcription of mouse bestrophin-1, TMEM16A, or actin mRNA. Samples containing reverse-transcriptase (RT; +) or negative controls lacking RT (−) are included for each tissue/primer combination. *500 bp Indicates a marker of 500 bp. The specificity of all primer sets was checked by sequencing of resultant PCR products.

cells would be low. Mouse brain and kidney cDNA were run in parallel as positive controls. We detected TMEM16A and bestrophin-1 mRNA expression in mouse brain, kidney, and mpkCCD$_{c14}$ cell lysates (Fig. 10).

AVP increases the concentration of extracellular ATP at the apical surface of mpkCCD$_{c14}$ cells. Our findings suggest that ATP stimulates CACC-mediated Cl^- absorption in mpkCCD$_{c14}$ cells under conditions of aldosterone stimulation. To identify associated conditions that might increase extracellular ATP concentration, we evaluated whether AVP increases ATP concentration at the apical surface of mpkCCD$_{c14}$ cells. AVP has recently been shown to induce nucleotide secretion from isolated, perfused mouse cortical collecting duct (13). We administered vehicle control or AVP (10^{-9} M) to the basal side of mpkCCD$_{c14}$ cells and compared the ATP concentrations at the apical surface of both groups of cells. We found that AVP induced a 56.5 ± 17% increase in ATP concentration at the apical surface of cell monolayers (Fig. 11), indicating that AVP can increase apical ATP concentration in cortical collecting duct cells.

DISCUSSION

In this study, we used the mpkCCD$_{c14}$ cell line to examine the relationship between ATP-mediated regulation of ENaC and CACC activity in cortical collecting duct cells. We found that there were two distinct dose-response profiles for the ATP I_{sc} response. At concentrations between 10^{-5} and 10^{-4} M, ATP induced a multiphasic response consisting of an initial transient peak, a second lower peak, followed by a sustained decrease in I_{sc}. This sustained decrease in I_{sc}, which fell below baseline I_{sc}, represents ATP-mediated inhibition of ENaC because amiloride treatment eliminated the sustained decrease in I_{sc}. At concentrations between 10^{-7} and 10^{-6} M, ATP only stimulated a transient peak in I_{sc}. Interestingly, the direction of this peak current response was voltage dependent. When mpkCCDc14 cell monolayers were clamped to a V_{te} below −10 mV, ATP stimulated an increase in negative clamp current. Thus, when cells were clamped to a V_{te} of −50 mV, the V_{te} across aldosterone-stimulated mpkCCD$_{c14}$ cells, ATP also induced an increase in negative clamp current.

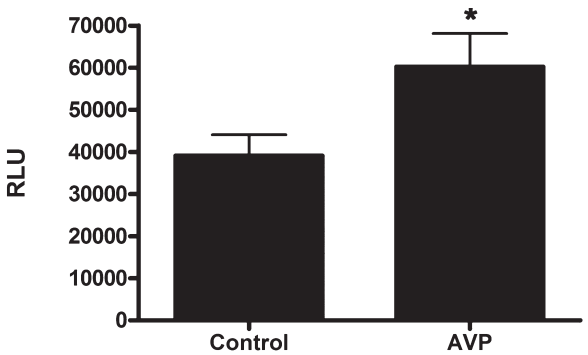

Fig. 11. Arginine vasopressin (AVP) increases ATP concentration at the apical membrane of mpkCCD$_{c14}$ cells. Media from the apical side of cell monolayers were replaced with PBS. Vehicle control or AVP (10^{-9} M) was added to the basal side of cell monolayers. PBS was collected, and ATP concentrations were measured using an ATP determination kit. Luminometer readings are reported in relative light units (RLU; $n = 11$ filters each). *$P < 0.05$.

We conclude that this increase in negative current represents an increase in Cl^- absorption through CACC. Several lines of evidence support this conclusion. First, the macroscopic current-voltage relationship for ATP-inducible current demonstrates that when cells are clamped to a V_{te} of 0 mV, a condition in which passive transport is eliminated, the ATP response is not eliminated. This finding suggests that ATP does not simply induce a change in passive transport but rather a change in active transport. Second, in ion substitution experiments, when Cl^- was substituted with gluconate, I_{clamp}^{ATP} was significantly inhibited; when Cl^- was substituted with sulfate, I_{clamp}^{ATP} was abolished. These experiments indicate that Cl^- is the predominant anion involved in I_{clamp}^{ATP}; furthermore, the small residual ATP response when Cl^- was substituted with gluconate may reflect ATP-mediated stimulation of gluconate transport through CACC (18). Third, suramin, BAPTA-AM, and FFA could inhibit I_{clamp}^{ATP}, strongly suggesting that ATP activates P2Y receptors and signals through intracellular calcium to stimulate CACC.

Our data are also supported by the original findings by Cuffe and colleagues (6), who showed in M1 cortical collecting duct cells that ATP stimulates Cl^- secretion through CACC. In this study, the authors characterized the same Cl^- transport machinery that is present in mpkCCD$_{c14}$ cells, but they performed these studies under short-circuit conditions. Our findings demonstrate that ATP stimulates Cl^- absorption through CACC when cells are clamped to a V_{te} less than −10 mV, which may operate under conditions of aldosterone stimulation. Our studies expand the current understanding of CACC function in the kidney by considering the relationship between aldosterone and purinergic signaling pathways in regulating Cl^- transport.

We propose that the status of ENaC activity, by controlling V_{te}, dictates the direction of ATP-stimulated Cl^- transport via CACC in cortical collecting duct cells. Extracellular nucleotides can act as paracrine hormones that are released by renal

epithelial cells in different physiological contexts. Recent studies demonstrated that urinary ATP production increases with high-NaCl feeding; this increase in ATP stimulates the $P2Y_2$ receptor system in the cortical collecting duct to inhibit ENaC activity (16, 17, 22). Since high-dietary NaCl intake leads to ECF volume expansion, serum aldosterone levels are suppressed, and as a consequence, ENaC activity is further diminished. Thus, with high-dietary NaCl intake, ATP would stimulate Cl^- secretion via CACC in cortical collecting duct cells because ENaC activity would be maximally inhibited. This mechanism could contribute to enhancing net urinary NaCl excretion under conditions of ECF volume expansion.

ATP production in cortical collecting duct cells may also increase under conditions where AVP levels are elevated. Using a biosensor approach, Odgaard and colleagues (13) demonstrated that AVP induces nucleotide secretion from isolated, perfused mouse cortical collecting duct, with an apparent peak nucleotide concentration of 300 nM. We also found that AVP stimulated an increase in ATP concentration at the apical side of $mpkCCD_{c14}$ cells. With severe volume depletion, both aldosterone and AVP levels are elevated so that NaCl absorption in the cortical collecting duct is maximally enhanced. We suggest that AVP-mediated increases in local ATP concentration in cortical collecting duct cells, in the context of maximal ENaC activity, would lead to an increase in Cl^- absorption through CACC. This is reminiscent of airway epithelia where cAMP increases Cl^- absorption through CFTR when ENaC activity is elevated (31). This pathway in cortical collecting duct cells could thus serve to enhance Cl^- absorption, in conjunction with Na^+ absorption, in states of severe volume depletion.

In this study, we primarily characterized the transient phase of the ATP response. Dr. Jens Leipziger's group demonstrated that the cortical collecting duct spontaneously releases extracellular ATP into the tubular lumen and that AVP stimulates rapid bursts of nucleotide secretion (13). They propose that repeated bursts of ATP release may meld into an integrated increase in intracellular Ca^{2+} concentration in the cortical collecting duct. We suggest that repeated bursts of ATP secretion into the tubular lumen of the collecting duct occur in both volume expansion and depletion, which may lead to repeated stimulation of CACC and significant changes in urinary Cl^- excretion over time. The relative contribution of this process to net urinary Cl^- excretion, under different states of ECF volume, will need to be confirmed in future in vivo studies.

In conclusion, we show that ATP stimulates CACC-mediated Cl^- absorption under conditions of aldosterone stimulation. These findings provide a framework for understanding the contexts under which ATP stimulates Cl^- absorption vs. secretion in cortical collecting duct cells. The direction of Cl^- transport is voltage dependent and dictated by the level of ENaC activity. With ECF volume expansion, ATP levels are elevated and ENaC activity is inhibited in cortical collecting duct cells so that ATP stimulates Cl^- secretion via CACC. With ECF volume depletion, ATP levels are also elevated but ENaC activity is simultaneously stimulated so that ATP stimulates Cl^- absorption via CACC. In both contexts, the interplay between aldosterone and purinergic signaling regulates NaCl transport in cortical collecting duct cells, which may ultimately contribute to the control of ECF volume status and blood pressure.

ACKNOWLEDGMENTS

We are grateful to Dr. Alain Vandewalle (Institut National de la Santé et de la Recherche Médicale) for providing $mpkCCD_{c14}$ cells for the experiments. We thank Dr. Tom Kleyman (University of Pittsburgh) for valuable discussions.

GRANTS

This work was supported by National Institutes of Health Grants K08-DK-073487 (to A. C. Pao) and T32-DK-7357-26A1 (to P. P. Kathpalia) and by Satellite Healthcare (2008 Norman S. Coplon Extramural Grant to A. C. Pao).

DISCLOSURES

No conflicts of interest, financial or otherwise, are declared by the author(s).

AUTHOR CONTRIBUTIONS

Author contributions: M.R. and A.C.P. conception and design of research; M.R. and P.P.K. performed experiments; M.R., P.P.K., and A.C.P. analyzed data; M.R., P.P.K., J.H.W., and A.C.P. interpreted results of experiments; M.R. and P.P.K. prepared figures; M.R. and A.C.P. drafted manuscript; M.R., P.P.K., J.H.W., and A.C.P. edited and revised manuscript; M.R., J.H.W., and A.C.P. approved final version of manuscript.

REFERENCES

1. **Barro Soria R, Spitzner M, Schreiber R, Kunzelmann K.** Bestrophin-1 enables Ca^{2+}-activated Cl^- conductance in epithelia. *J Biol Chem* 284: 29405–29412, 2009.
2. **Barro-Soria R, Schreiber R, Kunzelmann K.** Bestrophin 1 and 2 are components of the Ca^{2+} activated Cl^- conductance in mouse airways. *Biochim Biophys Acta* 1783: 1993–2000, 2008.
3. **Bens M, Vallet V, Cluzeaud F, Pascual-Letallec L, Kahn A, Rafestin-Oblin ME, Rossier BC, Vandewalle A.** Corticosteroid-dependent sodium transport in a novel immortalized mouse collecting duct principal cell line. *J Am Soc Nephrol* 10: 923–934, 1999.
4. **Bhalla V, Hallows KR.** Mechanisms of ENaC regulation and clinical implications. *J Am Soc Nephrol* 19: 1845–1854, 2008.
5. **Caputo A, Caci E, Ferrera L, Pedemonte N, Barsanti C, Sondo E, Pfeffer U, Ravazzolo R, Zegarra-Moran O, Galietta LJ.** TMEM16A, a membrane protein associated with calcium-dependent chloride channel activity. *Science* 322: 590–594, 2008.
6. **Cuffe JE, Bielfeld-Ackermann A, Thomas J, Leipziger J, Korbmacher C.** ATP stimulates Cl^- secretion and reduces amiloride-sensitive Na^+ absorption in M-1 mouse cortical collecting duct cells. *J Physiol* 524: 77–90, 2000.
7. **Davis AJ, Forrest AS, Jepps TA, Valencik ML, Wiwchar M, Singer CA, Sones WR, Greenwood IA, Leblanc N.** Expression profile and protein translation of TMEM16A in murine smooth muscle. *Am J Physiol Cell Physiol* 299: C948–C959, 2010.
8. **Dutta AK, Woo K, Doctor RB, Fitz JG, Feranchak AP.** Extracellular nucleotides stimulate Cl^- currents in biliary epithelia through receptor-mediated IP3 and Ca^{2+} release. *Am J Physiol Gastrointest Liver Physiol* 295: G1004–G1015, 2008.
9. **Fischer H, Illek B, Sachs L, Finkbeiner WE, Widdicombe JH.** CFTR and calcium-activated chloride channels in primary cultures of human airway gland cells of serous or mucous phenotype. *Am J Physiol Lung Cell Mol Physiol* 299: L585–L594, 2010.
10. **Grantham JJ, Wallace DP.** Return of the secretory kidney. *Am J Physiol Renal Physiol* 282: F1–F9, 2002.
11. **Hamm LL, Feng Z, Hering-Smith KS.** Regulation of sodium transport by ENaC in the kidney. *Curr Opin Nephrol Hypertens* 19: 98–105, 2010.
12. **Kunzelmann K, Kongsuphol P, Aldehni F, Tian Y, Ousingsawat J, Warth R, Schreiber R.** Bestrophin and TMEM16-Ca^{2+} activated Cl^- channels with different functions. *Cell Calcium* 46: 233–241, 2009.
13. **Odgaard E, Praetorius HA, Leipziger J.** AVP-stimulated nucleotide secretion in perfused mouse medullary thick ascending limb and cortical collecting duct. *J Med Invest* 56: 262–263, 2009.
14. **Park H, Oh SJ, Han KS, Woo DH, Mannaioni G, Traynelis SF, Lee CJ.** Bestrophin-1 encodes for the Ca^{2+}-activated anion channel in hippocampal astrocytes. *J Neurosci* 29: 13063–13073, 2009.

15. **Petrukhin K, Koisti MJ, Bakall B, Li W, Xie G, Marknell T, Sandgren O, Forsman K, Holmgren G, Andreasson S, Vujic M, Bergen AA, McGarty-Dugan V, Figueroa D, Austin CP, Metzker ML, Caskey CT, Wadelius C.** Identification of the gene responsible for Best macular dystrophy. *Nat Genet* 19: 241–247, 1998.
16. **Pochynyuk O, Bugaj V, Rieg T, Insel PA, Mironova E, Vallon V, Stockand JD.** Paracrine regulation of the epithelial Na^+ channel in the mammalian collecting duct by purinergic P2Y2 receptor tone. *J Biol Chem* 283: 36599–36607, 2008.
17. **Pochynyuk O, Rieg T, Bugaj V, Schroth J, Fridman A, Boss GR, Insel PA, Stockand JD, Vallon V.** Dietary Na^+ inhibits the open probability of the epithelial sodium channel in the kidney by enhancing apical P2Y2-receptor tone. *FASEB J* 24: 2056–2065, 2010.
18. **Qu Z, Hartzell HC.** Anion permeation in Ca^{2+}-activated Cl^- channels. *J Gen Physiol* 116: 825–844, 2000.
19. **Rajagopal M, Fischer H, Widdicombe JH.** Hormonal and purinergic stimulation of bicarbonate secretion in oviducts of rhesus monkey. *Am J Physiol Endocrinol Metab* 295: E55–E62, 2008.
20. **Rajagopal M, Kathpalia PP, Thomas SV, Pao AC.** Activation of P2Y1 and P2Y2 receptors induces chloride secretion via calcium-activated chloride channels in kidney inner medullary collecting duct cells. *Am J Physiol Renal Physiol* 301: F544–F553, 2011.
21. **Rajagopal M, Pao AC.** Adenosine activates a2b receptors and enhances chloride secretion in kidney inner medullary collecting duct cells. *Hypertension* 55: 1123–1128, 2010.
22. **Rieg T, Bundey RA, Chen Y, Deschenes G, Junger W, Insel PA, Vallon V.** Mice lacking P2Y2 receptors have salt-resistant hypertension and facilitated renal Na^+ and water reabsorption. *FASEB J* 21: 3717–3726, 2007.
23. **Schroeder BC, Cheng T, Jan YN, Jan LY.** Expression cloning of TMEM16A as a calcium-activated chloride channel subunit. *Cell* 134: 1019–1029, 2008.
24. **Sonnenberg H.** Secretion of salt and water into the medullary collecting duct of Ringer-infused rats. *Am J Physiol* 228: 565–568, 1975.
25. **Soundararajan R, Pearce D, Hughey RP, Kleyman TR.** Role of epithelial sodium channels and their regulators in hypertension. *J Biol Chem* 285: 30363–30369, 2010.
26. **Stokes JB.** Physiologic resistance to the action of aldosterone. *Kidney Int* 57: 1319–1323, 2000.
27. **Stokes JB, Tisher CC, Kokko JP.** Structural-functional heterogeneity along the rabbit collecting tubule. *Kidney Int* 14: 585–593, 1978.
28. **Stoner LC, Burg MB, Orloff J.** Ion transport in cortical collecting tubule; effect of amiloride. *Am J Physiol* 227: 453–459, 1974.
29. **Terada Y, Knepper MA.** Thiazide-sensitive NaCl absorption in rat cortical collecting duct. *Am J Physiol Renal Fluid Electrolyte Physiol* 259: F519–F528, 1990.
30. **Thomas SV, Kathpalia PP, Rajagopal M, Charlton C, Zhang J, Eaton DC, Helms MN, Pao AC.** Epithelial sodium channel regulation by cell surface-associated serum- and glucocorticoid-regulated kinase 1. *J Biol Chem* 286: 32074–32085, 2011.
31. **Uyekubo SN, Fischer H, Maminishkis A, Illek B, Miller SS, Widdicombe JH.** cAMP-dependent absorption of chloride across airway epithelium. *Am J Physiol Lung Cell Mol Physiol* 275: L1219–L1227, 1998.
32. **Wallace DP, Rome LA, Sullivan LP, Grantham JJ.** cAMP-dependent fluid secretion in rat inner medullary collecting ducts. *Am J Physiol Renal Physiol* 280: F1019–F1029, 2001.
33. **Yang YD, Cho H, Koo JY, Tak MH, Cho Y, Shim WS, Park SP, Lee J, Lee B, Kim BM, Raouf R, Shin YK, Oh U.** TMEM16A confers receptor-activated calcium-dependent chloride conductance. *Nature* 455: 1210–1215, 2008.
34. **Zhang Y, Listhrop R, Ecelbarger CM, Kishore BK.** Renal sodium transporter/channel expression and sodium excretion in P2Y2 receptor knockout mice fed a high-NaCl diet with/without aldosterone infusion. *Am J Physiol Renal Physiol* 300: F657–F668, 2011.
35. **Zsembery A, Fortenberry JA, Liang L, Bebok Z, Tucker TA, Boyce AT, Braunstein GM, Welty E, Bell PD, Sorscher EJ, Clancy JP, Schwiebert EM.** Extracellular zinc and ATP restore chloride secretion across cystic fibrosis airway epithelia by triggering calcium entry. *J Biol Chem* 279: 10720–10729, 2004.